

Multilevel Bayesian Deep Neural Networks

BY NEIL K. CHADA¹, AJAY JASRA¹, KODY J. H. LAW² & SUMEETPAL S. SINGH³

¹Applied Mathematics and Computational Science Program, Computer, Electrical and Mathematical Sciences and Engineering Division, King Abdullah University of Science and Technology, Thuwal, 23955-6900, KSA. E-Mail:

ajay.jasra@kaust.edu.sa, neilchada123@gmail.com

²Department of Mathematics, University of Manchester, Manchester, M13 9PL, UK. E-Mail: *kody.law@manchester.ac.uk*

³Department of Engineering, University of Cambridge, Cambridge, CB2 1PZ, UK. E-Mail: *sss40@cam.ac.uk*

Abstract

In this article we consider Bayesian inference associated to deep neural networks (DNNs) and in particular, trace-class neural network (TNN) priors which were proposed by Sell et al. [43]. Such priors were developed as more robust alternatives to classical architectures in the context of inference problems. For this work we develop multilevel Monte Carlo (MLMC) methods for such models. MLMC is a popular variance reduction technique, with particular applications in Bayesian statistics and uncertainty quantification. We show how a particular advanced MLMC method that was introduced in [6] can be applied to Bayesian inference from DNNs, and used to compute expectations associated to the posterior predictive. We establish that the cost to achieve a given mean square error can be reduced by several orders, in comparison to more conventional techniques. To verify such results we provide numerous numerical experiments on several model problems arising in machine learning, including regression, classification, and reinforcement learning.

Keywords: Deep Neural Networks, Multilevel Monte Carlo, Sequential Monte Carlo, Trace-Class, Reinforcement Learning

AMS subject classifications: 62M20, 62M45, 62F15, 93E35

1 Introduction

Machine learning [7, 35, 39] has emerged as a topic of interest, in a wide class of mathematical and statistical disciplines. This is largely due to the amount of machinery available in terms of advanced numerical algorithms, but also the amount of readily available data. Common examples of machine learning tasks, or methodologies, include clustering, classification and reinforcement learning. Typically many of these methodologies aim to optimize a function, which is used for learning and prediction purposes, such as image processing, handwriting recognition and natural language processing. These problems are often solved with deterministic methods, based on variational techniques. The Bayesian paradigm involves formulating a consistent probabilistic model, and then identifying the posterior distribution of the quantity of interest given the data, hence providing predictions with quantified uncertainty, a crucial feature which is often lacking in widely used mainstream methods and can lead to catastrophic failure [25, 37]. The Bayesian approach often provides an elegant and well-defined solution, in theory, and it is widely accepted that this is often a “gold-standard” to strive for. However, most existing methodology is simply too computationally expensive to consider for practical applications, and so one ordinarily relies on variational approximations, which are no longer consistent [8, 16, 17]. In this paper our focus is on *fully Bayesian inference* for deep learning, through the aid and use of advanced stochastic algorithms, which have been exploited for Monte Carlo (MC) simulation. Before describing in detail our contributions, we first present a general literature overview on this entities, and how they are related to Bayesian machine learning [24, 40].

Monte Carlo methods [9] are well-known class of methods aimed to solve stochastic computation problems. Such developments have been primarily in the fields of computational physics, statistics and numerical analysis. In particular one methodology which improves on vanilla MC is that of multilevel Monte Carlo (MLMC). MLMC aims to reduce the computational cost, and complexity, to attain a particular order of mean square error (MSE), i.e. $\mathcal{O}(\varepsilon^2)$ for $\varepsilon > 0$. First introduced in [18, 19, 26] and primarily applied to diffusion processes in mathematical finance, it has seen since since various extensions to other

fields. Related to this work, it has been applied to MC methods within computational statistics which includes sequential Monte Carlo (SMC), Markov Chain Monte Carlo (MCMC) [5, 6, 27, 30, 31] and other related methods, based on sampling from a distribution of interest. However in terms of the application of MLMC to machine learning, there has been limited work on this. Notable works along this direction include the improvement of complexity in gradient estimators within variational inference [15, 44], and improved complexity for data-driven surrogate modelling of high-dimensional PDE and SDE models [14, 20, 34]. However as of yet this has not been exploited for the use of statistical inference problems in machine learning.

Deep neural networks (DNNs) [22] are a popular and powerful parametric model class which can be used for solving a variety of machine learning problems. These architectures are highly applicable to a wide array of disciplines and applications, where a major advantage of DNNs is that one attains the universal approximation theorem, which in brief states that the NN can approximate a wide class of target functions [2, 3, 28]. For this work our interest in DNNs are w.r.t. generating random processes. There has been extensive work on this connecting DNN with Gaussian and non-Gaussian processes [1, 33, 36, 40]. In the case of Deep Gaussian processes, which are no longer Gaussian, variational approaches are typically employed [32]. Deep Gaussian and α -stable process priors for fully Bayesian edge-preserving inversion have been employed in the context of inverse problems in [12, 13, 38], but these studies have typically been limited to low input dimensionality due to the debilitating computational complexity. Sell et al. introduce trace-class DNN (TNN) priors [43], which are non-stationary, non-Gaussian, and well-defined in the infinite-width limit, yet scale well with input dimension. For example, they have been successfully applied to problems with up to $n = 17$ dimensions. Our motivation in this manuscript is to provide a new methodology, multilevel Bayesian deep neural networks, which combines TNN prior models with an advanced MLSMC algorithm. This methodology combines the advantages of the TNN model in terms of scalability and flexibility, with the efficiency of MLSMC to achieve the canonical computational complexity of $1/\text{MSE}$. For problems of this form, where MC is used to simulate from an approximate distribution, such complexity can only be attained in a MLMC framework, and it is impossible to do better.

1.1 Contributions

Our contributions of this work are summarized through the following points.

- We show how to use MLMC in the context of Bayesian inference for deep neural networks. The specific method we use is multilevel sequential Monte Carlo (MLSMC) samplers [6]. Our motivation is to reduce the computational complexity, where we show it is possible to attain the canonical rate of convergence $\text{Cost} = \text{MSE}^{-1}$.
- We prove two key results within our work. First, we are able to derive strong rates of convergence for TNN priors in a multilevel setting. Secondly, we establish a bound on the MSE, which can be decomposed into a variance and bias term. By leveraging these two results, we establish that our method converges to the true underlying posterior with the canonical rate.
- Various numerical experiments are presented to verify the theoretical findings discussed above. This is related to both demonstrating that the strong convergence rate is attained, and also that the MLSMC sampler with TNN priors can reduce the cost to attain a particular order of MSE. The experiments are conducted on machine learning examples including regression, classification and reinforcement learning.

1.2 Outline

The outline of this article is structured as follows. In Section 2 we present preliminary material related to both the model problem and multilevel Monte Carlo. This leads onto Section 3, where we present our numerical algorithm coupled with our main mathematical result, which is a bound on the MSE establishing convergence of our method. We then discuss and introduce our multilevel trace-class priors in Section

4 where we demonstrate they attain the canonical rate of convergence, with numerical verification. In Section 5 our numerical results are presented on a range of machine learning tasks, verifying the improved gains on computational cost using the MLSMC sampler, combined with TNN priors. Finally we conclude, and remark on future directions, in Section 6. The proof of our main theorem is deferred to the Appendix.

2 Model Formulation

In this section we provide a preliminary background on the setting, and formulation of the model problem. This will include an initial discussion on our setup, which will discuss neural networks and how they related to Bayesian modeling, as well as introducing the key concepts of multilevel Monte Carlo.

Suppose we have data $\mathcal{D} = ((x_1, y_1), \dots, (x_N, y_N))$, $N \in \mathbb{N}$, where, for $i \in \{1, \dots, N\}$, $x_i \in \mathsf{X}$ and $y_i \in \mathsf{Y}$. The objective is to infer a predictive model $f : \mathsf{X} \rightarrow \mathsf{Y}$ based on the data. One way to do this is with a parametric model of the form $f : \mathsf{X} \times \Theta \rightarrow \mathsf{Y}$, with $\Theta \subseteq \mathbb{R}^{d_\theta}$. It is assumed that $x_{1:N}$ are deterministic. For some $m \in \mathbb{N}$, let

$$f : \mathsf{X} \times \Theta \rightarrow \mathbb{R}^m, \quad \text{with} \quad f(x, \theta) = (f_1(x, \theta), \dots, f_m(x, \theta)).$$

If $\mathsf{Y} = \mathbb{R}^m$, then we will assume that for $i \in \{1, \dots, N\}$

$$y_i = f(x_i, \theta) + \epsilon_i, \quad \epsilon_i \stackrel{\text{ind}}{\sim} \mathcal{N}_m(0, \Sigma_i), \quad (2.1)$$

where ind denotes independence across the indices $i \in \{1, \dots, N\}$ and $\mathcal{N}_m(\mu, \Sigma)$ denotes the m -dimensional Gaussian distribution with mean μ and covariance matrix Σ .

On the other hand, if $\mathsf{Y} = \{1, \dots, m\}$, then we define the so-called *softmax* function as

$$h_k(x, \theta) := \frac{\exp\{f_k(x, \theta)\}}{\sum_{j=1}^K \exp\{f_j(x, \theta)\}}, \quad k \in \mathsf{Y}, \quad (2.2)$$

and assume that $y_i \sim h(x_i)$, independently for $i \in \{1, \dots, N\}$, where $h(x) = (h_1(x), \dots, h_m(x))$ denotes a categorical distribution on m outcomes, given input x .

A popular parametric model is deep neural networks (DNN) [22]. In this scenario, affine functions are composed with simple element-wise *activation functions* $\nu : \mathbb{R} \rightarrow \mathbb{R}$. We make the definition that for $k \in \mathbb{N}$ given and $z_{1:k} \in \mathbb{R}^k$, $\sigma_k : \mathbb{R}^k \rightarrow \mathbb{R}^k$ with $\sigma_k(z_{1:k}) = (\nu(z_1), \dots, \nu(z_k))^\top$. An example is $\nu(z) = \max\{0, z\}$ for $z \in \mathbb{R}_+$, the so-called *ReLU activation*. Let $\mathsf{X} = \mathbb{R}^n$ and $\mathsf{Y} = \mathbb{R}^m$. The DNN itself can be defined in the following way. Let $D \in \mathbb{N}$, $(n_0, \dots, n_D) \in \mathbb{N}^{D+1}$ be given, with the constraint that $n_0 = n$ for the input layer and $n_D = m$ for the output layer. Now for weights $A_d \in \mathbb{R}^{n_d \times n_{d-1}}$ and biases $b_d \in \mathbb{R}^{n_d}$, $d \in \{1, \dots, D\}$ also given, we use the notation $\theta := ((A_1, b_1), \dots, (A_D, b_D))$ and so $\theta \in \Theta = \bigotimes_{d=1}^D \{\mathbb{R}^{n_d \times n_{d-1}} \times \mathbb{R}^{n_d}\}$. Now set

$$\begin{aligned} g_0(x, \theta) &:= A_1 x + b_1, \\ g_d(x, \theta) &:= A_d \sigma_{n_d} (g_{d-1}(x)) + b_d, \quad d \in \{1, \dots, D-1\}, \\ f(x, \theta) &:= A_D \sigma_{n_D} (g_{D-1}(x)) + b_D, \end{aligned} \quad (2.3)$$

where $f(x, \theta)$ is the output of the final layer of the DNN. For any given $f(x, \theta)$ and parameter space Θ one can place a prior $\bar{\pi}$ on Θ . Given the structure in (2.1) one then has a posterior

$$\pi(\theta | y_{1:N}) \propto p(y_{1:N} | \theta, x_{1:N}) \bar{\pi}(\theta), \quad (2.4)$$

assuming it is well-defined. In the case of regression (2.1), the likelihood function is

$$p(y_{1:N} | \theta, x_{1:N}) = \prod_{i=1}^N \phi_m(y_i; f(x_i, \theta), \Sigma_i), \quad (2.5)$$

where $\phi_m(y; \mu, \Sigma)$ is the m -dimensional Gaussian density of mean μ , covariance Σ evaluated at y given. In the case of classification (2.2), the likelihood function is

$$p(y_{1:N}|\theta, x_{1:N}) = \prod_{i=1}^N \prod_{k=1}^m h_k(x_i, \theta)^{\mathbb{I}_{[y_i=k]}}, \quad (2.6)$$

where $\mathbb{I}_{[y_i=k]} = 1$ if $y_i = k$ and 0 otherwise.

2.1 Multilevel Bayesian Neural Networks

We shall begin with a short review of MLMC. Let us assume that we are given a probability density Ψ , on a state-space \mathbf{U} and it is of interest to compute expectations of Ψ -integrable functions, $\varphi : \mathbf{U} \rightarrow \mathbb{R}$; $\Psi(\varphi) := \int_{\mathbf{U}} \varphi(u) \Psi(u) du$ with du a dominating σ -finite measure (often Lebesgue). Now, we assume that working with Ψ is not computationally feasible (e.g. has an infinite computational cost) but there exist a scalar parameter $l \in \mathbb{N}_0 = \{0\} \cup \mathbb{N}$ which parameterises an approximation Ψ_l of Ψ , where Ψ_l a density on a state-space $\mathbf{U}_l \subseteq \mathbf{U}$ such that:

1. For any $\varphi : \mathbf{U} \rightarrow \mathbb{R}$ that is both Ψ_l and Ψ -integrable we have $\lim_{l \rightarrow \infty} \Psi_l(\varphi) = \Psi(\varphi)$, where $\Psi_l(\varphi) = \int_{\mathbf{U}} \varphi(u) \Psi_l(u) du$.
2. The cost of computing with Ψ_l is increasing in l .

Let $L \in \mathbb{N}$ be given, we have the telescoping sum identity

$$\Psi_L(\varphi) = \Psi_0(\varphi) + \sum_{l=1}^L [\Psi_l - \Psi_{l-1}](\varphi), \quad (2.7)$$

with $[\Psi_l - \Psi_{l-1}](\varphi) = \Psi_l(\varphi) - \Psi_{l-1}(\varphi)$. The idea behind MLMC is to try and approximate the R.H.S. of (2.7) in such a way as to reduce the cost of a particular order of mean square error (MSE) versus approximating the L.H.S. of (2.7). The way in which this is achieved is to construct couplings of (Ψ_l, Ψ_{l-1}) , $l \in \{1, \dots, L\}$, that is, joint densities $\check{\Psi}_l$, on $\mathbf{U}_l \times \mathbf{U}_{l-1}$ such that $\int_{\mathbf{U}_l} \check{\Psi}_l(u_l, u_{l-1}) du_l = \Psi_{l-1}(\tilde{u}_{l-1})$ and $\int_{\mathbf{U}_{l-1}} \check{\Psi}_l(u_l, u_{l-1}) du_{l-1} = \Psi_l(u_l)$.

The MLMC estimator can be constructed in the following way.

1. Sample $U_0^1, \dots, U_0^{P_0}$ i.i.d. from Ψ_0 , with $P_0 \in \mathbb{N}$ given.
2. For $l \in \{1, \dots, L\}$ independently of all other random variables, sample $(U_l^1, \tilde{U}_{l-1}^1), \dots, (U_l^{P_l}, \tilde{U}_{l-1}^{P_l})$ i.i.d. from $\check{\Psi}_l$, with $P_l \in \mathbb{N}$ given.

Then, we have the approximation

$$\Psi_L^{ML}(\varphi) := \frac{1}{P_0} \sum_{i=1}^{P_0} \varphi(U_0^i) + \sum_{l=1}^L \frac{1}{P_l} \sum_{i=1}^{P_l} \{\varphi(U_l^i) - \varphi(\tilde{U}_{l-1}^i)\}. \quad (2.8)$$

Now, alternatively, one can use i.i.d. samples U_L^1, \dots, U_L^P from Ψ_L to approximate $\Psi_L(\varphi)$:

$$\Psi_L^{ID}(\varphi) := \frac{1}{P} \sum_{i=1}^P \varphi(U_L^i), \quad (2.9)$$

In either scenario one would have a standard, variance (assuming it exists) plus square bias decomposition of the MSE; e.g. for the MLMC estimator:

$$\mathbb{E}[(\Psi_L^{ML}(\varphi) - \Psi(\varphi))^2] = \text{Var}[\Psi_L^{ML}(\varphi)] + [\Psi_L - \Psi](\varphi)^2, \quad (2.10)$$

with Var representing the variance operator. The bias is of course the same for both estimators (2.8) and (2.9) and so, if there is to be an advantage for using (2.8) under an MSE criterion, it would be via the variance. The variance of (2.8) is

$$\text{Var}[\Psi_L^{ML}(\varphi)] = \frac{\text{Var}[\varphi(U_0^1)]}{P_0} + \sum_{l=1}^L \frac{\text{Var}[\varphi(U_l^1) - \varphi(U_{l-1}^1)]}{P_l},$$

whereas for (2.9)

$$\text{Var}[\Psi_L^{IID}(\varphi)] = \frac{\text{Var}[\varphi(U_L^1)]}{P}.$$

Now, if the couplings $\check{\Psi}_l$ are constructed so that $\text{Var}[\varphi(U_l^1) - \varphi(U_{l-1}^1)]$ falls sufficiently quickly with l then it can be possible to achieve an MSE (as in (2.10)) for the estimator (2.8) which is of the same order as (2.9) except for a cost that is lower. This is characterized in the following result. Below $\text{Cost}(\check{\Psi}_l)$ is the cost of one sample from $\check{\Psi}_l$.

Theorem 2.1 (Giles [18]). *Suppose that there exists constants $(\alpha, \beta, \gamma) \in \mathbb{R}_+^3$ with $\alpha \geq \frac{\min(\beta, \gamma)}{2}$ such that*

- (i) $|\Psi_l(\varphi) - \Psi(\varphi)| = \mathcal{O}(2^{-\alpha l})$.
- (ii) $\text{Var}[\varphi(U_l^1) - \varphi(U_{l-1}^1)] = \mathcal{O}(2^{-\beta l})$.
- (iii) $\text{Cost}(\check{\Psi}_l) = \mathcal{O}(2^{\gamma l})$.

Then for any $\varepsilon < 1$ and $L := \lceil \log(1/\varepsilon) \rceil$, there exists $(P_0, \dots, P_L) \in \mathbb{N}^{L+1}$ such that

$$\text{MSE} = \mathbb{E}[(\Psi_L^{ML}(\varphi) - \Psi(\varphi))^2] = \mathcal{O}(\varepsilon^2),$$

and

$$\text{Cost}(\text{MLMC}) := \sum_{l=0}^L P_l C_l = \begin{cases} \mathcal{O}(\varepsilon^{-2}), & \text{if } \beta > \gamma, \\ \mathcal{O}(\varepsilon^{-2}(\log \varepsilon)^2), & \text{if } \beta = \gamma, \\ \mathcal{O}(\varepsilon^{-2 - \frac{\gamma - \beta}{\alpha}}), & \text{if } \beta < \gamma. \end{cases} \quad (2.11)$$

We remark that the cost in (2.11) can be lower than that of using the estimator (2.9), depending upon the parameters (α, β, γ) , and simultaneously, the estimator (2.11) having an MSE of $\mathcal{O}(\varepsilon^2)$. The case of $\beta > \gamma$ is referred to as the canonical rate of convergence, i.e. $\mathcal{O}(\varepsilon^{-2})$, since this is the best rate that one can obtain (as such we sometimes refer to this as ‘‘optimal’’, despite that this terminology is typically avoided since all 3 rates in (2.11) are optimal for the given case). In the original work of Giles [18] the methodology of MLMC was motivated and applied to diffusion processes with applications in financial mathematics. In [18], $\beta \in \mathbb{R}$ relates to the strong rate of convergence, and $\alpha \in \mathbb{R}$ the weak rate of convergence. In our context, as we do not work with diffusion processes, not only is strong and weak convergence not required, i.i.d. sampling of couplings is not achievable in our context (to be defined below) and thus an alternative methodology to reducing the variance of the higher level l differences are required.

2.1.1 Multilevel Neural Networks

We now consider the question of choosing the dimension of θ , in particular n_d for $d \in \{1, \dots, D-1\}$ (since n_0 and n_D are fixed to the input and output dimensions). For simplicity, here we assume D is fixed and the NN width is the same for all layers other than the input or the output, i.e. $n_d = n_{d'}$ for $d, d' \in \{1, \dots, D-1\}$, but dependent upon some resolution parameter $l \in \mathbb{N}$. We can now re-define $n_l = 2^l$, noting that $n_0 = n$ and $n_D = m$, so those variables are no longer needed. We will denote the corresponding vector of parameters by $\theta_l := ((A_1^l, b_1^l), \dots, (A_D^l, b_D^l))$, with prior $\bar{\pi}_l(\theta_l)$, and the parameter space is $\Theta_l = \{\mathbb{R}^{n_l \times n} \times \mathbb{R}^{n_l}\} \otimes \{\mathbb{R}^{n_l \times n_l} \times \mathbb{R}^{n_l}\}^{\otimes D-2} \otimes \{\mathbb{R}^{m \times n_l} \times \mathbb{R}^m\}$, thus $\theta_l \in \Theta_l$. The NN’s output

function $g_D(x, \theta)$ (see (2.3)) for resolution l is denoted by $f_l(x, \theta_l)$, the likelihood by $p_l(y_{1:N}|\theta_l, x_{1:N})$, and the posterior distribution by

$$\pi_l(\theta_l|x_{1:N}, y_{1:N}) \propto p_l(y_{1:N}|\theta_l, x_{1:N})\bar{\pi}_l(\theta_l), \quad (2.12)$$

where $p_l(y_{1:N}|\theta_l, x_{1:N})$ is the likelihood function using θ_l parameters as in (2.5), and (2.6) for the second example discussed. We view this posterior (and the corresponding $f_l(x, \theta_l)$) as a finite approximation of the posterior associated to the non-parametric limiting DNN as $l \rightarrow \infty$, assuming it exists, and denoted π_* .

3 Algorithm and Main Result

In this section we introduce our methodology related to the Bayesian machine learning tasks, which we numerically test in Section 5. Namely we consider the ML sequential Monte Carlo method, and present it in our given framework. This will lead to the our main mathematical result, which is the convergence of our ML estimator, provided in terms of a bound on the MSE.

We begin this section by firstly presenting our algorithm for approximating quantities such as, for $(x, L) \in \mathbf{X} \times \mathbb{N}$ given:

$$\mathbb{E}_{\pi_L}[f_L(x, \theta_L)],$$

as well as some mathematical results which justify their implementation. The choice of posterior predictive expectation as a quantity of interest is motivated by the goal of our inference procedure, i.e. to make predictions related to the output of the neural network f . The form of our results are such that they extend trivially to objective functions $\varphi \circ f$, for Lipschitz φ , for example. We note that there are other possible test functions one can consider beyond the neural network. However we aim to explore this for future work. Our main objective is to construct a multilevel Monte Carlo estimator:

$$\mathbb{E}_{\pi_L}[f_L(x, \theta_L)] = \sum_{l=2}^L \{\mathbb{E}_{\pi_l}[f_l(x, \theta_l)] - \mathbb{E}_{\pi_{l-1}}[f_{l-1}(x, \theta_{l-1})]\} + \mathbb{E}_{\pi_1}[f_1(x, \theta_1)], \quad (3.1)$$

by approximating each summand on the R.H.S., as well as $\mathbb{E}_{\pi_1}[f_1(x, \theta_1)]$, using a suitable simulation method. Then we will show that the computational cost for doing so, versus, simply approximating $\mathbb{E}_{\pi_L}[f_L(x, \theta_L)]$ can be lower, when seeking to achieve a pre-specified mean square error.

3.1 Algorithm

The approach we construct follows that in [5, 6] and in order to directly invoke some its results, we introduce additional notation. Throughout this exposition $(x, L) \in \mathbf{X} \times \mathbb{N}$ are fixed and given. Let $l \in \{0, \dots, L-1\}$ and set $\mathbf{E}_l = \Theta_{l+1}$. For $l \in \{2, \dots, L\}$, we will write $\theta_l = (\theta_{l-1}, \tilde{\theta}_l)$, where $\tilde{\theta}_l \in \Theta_l \setminus \Theta_{l-1}$, also set $\theta_1 = \tilde{\theta}_1 \in \Theta_1$. We seek to connect these model notations to that used in Feynman-Kac formulae, so we will define for $l \in \{0, \dots, L-1\}$:

$$u_l := (\tilde{\theta}_1, \dots, \tilde{\theta}_{l+1}) = (u_{l-1}, \tilde{\theta}_{l+1}) \in \mathbf{E}_l,$$

and note that $u_l = \theta_{l+1}$. We will suppress the data $(x_{1:N}, y_{1:N})$ from the notation and set for $l \in \{1, \dots, L\}$

$$\pi_l(\theta_l) \propto p_l(y_{1:N}|\theta_l)\bar{\pi}_l(\theta_l) =: \kappa_{l-1}(u_{l-1}).$$

For any $l \in \{2, \dots, L\}$ and $\theta_{l-1} \in \Theta_{l-1}$, let $q_l(\cdot|\theta_{l-1})$ be a positive probability density on $\Theta_l \setminus \Theta_{l-1}$ and $q_1(u_0)$ a positive probability density on \mathbf{E}_0 . Set $G_0(u_0) = \kappa_0(u_0)/q_0(u_0)$ and for $l \in \{1, \dots, L-1\}$

$$G_l(u_l) = \frac{\kappa_l(u_l)}{\kappa_{l-1}(u_{l-1})q_{l+1}(\tilde{\theta}_{l+1}|\theta_l)}.$$

Let $(K_l)_{l \in \{1, \dots, L-1\}}$ be a sequence of $(\pi_l)_{l \in \{1, \dots, L-1\}}$ -invariant Markov kernels and define

$$M_l(u_{l-1}, du_l) = K_l(u_{l-1}, du'_l) q_{l+1}(\tilde{\theta}_{l+1} | u'_l) d\tilde{\theta}_{l+1}, \quad (3.2)$$

where $u_l = (u'_{l-1}, \tilde{\theta}_{l+1})$ and $d\tilde{\theta}_{l+1}$ is the appropriate dimensional Lebesgue measure. This kernel is invoked in Step 3 of Algorithm 1.

We are now in a position to define our algorithm which can approximate expectations w.r.t. the sequence of posteriors $(\pi_l)_{l \in \{1, \dots, L-1\}}$ and this is given in Algorithm 1. We introduce the ‘predictors’ $\eta_l(u_l) = \pi_l(u_{l-1}) q_{l+1}(\tilde{\theta}_{l+1} | u_{l-1})$, with $\eta_0(u_0)$ being the prior $q_1(u_0)$, which are computed by Algorithm 1. We will describe below how samples from these predictors this can be used to approximate the multilevel identity (3.1). Let $l \in \{1, \dots, L-1\}$, $\varphi_l : \Theta_l \rightarrow \mathbb{R}$ be π_l -integrable; we use the short-hand $\pi_l(\varphi_l) = \int_{\Theta_l} \varphi_l(\theta_l) \pi_l(\theta_l) d\theta_l$. Now writing the P_l -empirical measure of the samples $U_l^1 = ((u'_{l-1})^1, \tilde{\theta}_{l+1}^1), \dots, U_l^{P_l} = ((u'_{l-1})^{P_l}, \tilde{\theta}_{l+1}^{P_l})$ from Step 3 of Algorithm 1 as $\eta_l^{P_l}$, to approximate $\pi_l(\varphi_l)$ we can use

$$\pi_l^{P_l}(\varphi_l) := \frac{1}{P_l} \sum_{i=1}^{P_l} \varphi_l((u'_{l-1})^i) = \eta_l^{P_l}(\varphi_l), \quad (3.3)$$

where one should recall the notation in (3.4) given in Algorithm 1 and, as a convention, we will use $\eta_l^{P_l}(\varphi_l)$ instead of $\pi_l^{P_l}(\varphi_l)$ from herein. This estimate can be justified in the sense that there are formal results which prove that $\eta_l^{P_l}(\varphi_l)$ will converge to $\pi_l(\varphi_l)$, for instance, almost surely as $P_l \rightarrow +\infty$; see for instance [9].

Algorithm 1 Multilevel Sequential Monte Carlo Sampler for Deep Neural Networks.

1. **Input:** $L \in \mathbb{N}$ the highest resolution and the number of samples at each level $(P_0, \dots, P_{L-1}) \in \mathbb{N}^L$, with $+\infty > P_0 \geq P_1 \geq \dots \geq P_{L-1} \geq 1$.
2. **Initialize:** Sample $(U_0^1, \dots, U_0^{P_0})$ i.i.d. from $q_1(u_0)$. Set $\eta_0^{P_0} = P_0^{-1} \sum_{i=1}^{P_0} \delta_{U_0^i}(du_0)$, $l = 1$ and go to step 3..
3. **Iterate:** If $l = L$ stop. Otherwise for $i \in \{1, \dots, P_l\}$ sample $U_l^i | u_{l-1}^1, \dots, u_{l-1}^{P_{l-1}}$ independently using:

$$\sum_{j=1}^{P_{l-1}} \frac{G_{l-1}(u_{l-1}^j)}{\sum_{s=1}^{P_{l-1}} G_{l-1}(u_{l-1}^s)} M_l(u_{l-1}^j, \cdot).$$

Let $\eta_l^{P_l}$ denote the empirical measure of $\{U_l^i\}_{i=1}^{P_l}$ (see (3.3)). We will use the notation

$$u_l^i = ((u'_{l-1})^i, \tilde{\theta}_{l+1}^i). \quad (3.4)$$

Set $l = l + 1$ and go to the start of step 3.

Now, recalling (3.1), our objective is to approximate the difference, for $(x, l) \in \mathbf{X} \times \mathbb{N}$:

$$\mathbb{E}_{\pi_l}[f_l(x, \theta_l)] - \mathbb{E}_{\pi_{l-1}}[f_{l-1}(x, \theta_{l-1})] =: \pi_l(f_l) - \pi_{l-1}(f_{l-1}),$$

where \mathbb{E}_{π_l} denotes expectation w.r.t. π_l . Now, we have the simple identity

$$\begin{aligned} \mathbb{E}_{\pi_l}[f_l(x, \theta_l)] - \mathbb{E}_{\pi_{l-1}}[f_{l-1}(x, \theta_{l-1})] &= \mathbb{E}_{\pi_{l-1} \otimes q_l} \left[\frac{\kappa_{l-1}(\theta_l) Z_{l-1}}{\kappa_{l-2}(\theta_{l-1}) q_l(\tilde{\theta}_l | \theta_{l-1}) Z_l} f_l(x, \theta_l) - f_{l-1}(x, \theta_{l-1}) \right] \\ &= \mathbb{E}_{\pi_{l-1} \otimes q_l} \left[\frac{Z_{l-1}}{Z_l} G_{l-1}(U_{l-1}) f_l(x, \theta_l) - f_{l-1}(x, \theta_{l-1}) \right], \end{aligned} \quad (3.5)$$

where $\mathbb{E}_{\pi_{l-1} \otimes q_l}$ denotes expectation w.r.t. $\pi_{l-1}(\theta_{l-1})q_l(\tilde{\theta}_l|\theta_{l-1})$ and for any $l \in \{1, \dots, L\}$ and $Z_l = \int_{\Theta_l} \kappa_{l-1}(\theta_l) d\theta_l$ is the normalizing constant. One can approximate the R.H.S. of (3.5) as

$$\frac{\eta_{l-1}^{P_{l-1}}(G_{l-1}f_l)}{\eta_{l-1}^{P_{l-1}}(G_{l-1})} - \eta_{l-1}^{P_{l-1}}(f_{l-1}).$$

The justification of this estimator is informally as follows. $\eta_{l-1}^{P_{l-1}}(f_{l-1})$ will converge (as $P_{l-1} \rightarrow \infty$ and under assumptions) to $\pi_{l-1}(f_{l-1})$, which justifies the second term. Then $\eta_{l-1}^{P_{l-1}}(G_{l-1})$ will converge to

$$\begin{aligned} \int_{\Theta_l} \pi_{l-1}(\theta_{l-1})q_l(\tilde{\theta}_l|\theta_{l-1}) \frac{\kappa_{l-1}(\theta_l)}{\kappa_{l-2}(\theta_{l-1})q_l(\tilde{\theta}_l|\theta_{l-1})} d\theta_l &= \frac{1}{Z_{l-1}} \int_{\Theta_l} \kappa_{l-1}(\theta_l) d\theta_l \\ &= \frac{Z_l}{Z_{l-1}}. \end{aligned}$$

Similarly $\eta_{l-1}^{P_{l-1}}(G_{l-1}f_l)$ converges to

$$\int_{\Theta_l} \pi_{l-1}(\theta_{l-1})q_l(\tilde{\theta}_l|\theta_{l-1}) \frac{\kappa_{l-1}(\theta_l)}{\kappa_{l-2}(\theta_{l-1})q_l(\tilde{\theta}_l|\theta_{l-1})} f_l(x, \theta_l) d\theta_l.$$

which yields the appropriate identity on the R.H.S. of (3.5). As a result of this exposition, one can use the following approximation of $\pi_L(f_L)$:

$$\hat{\pi}_L(f_L) = \sum_{l=2}^L \left\{ \frac{\eta_{l-1}^{P_{l-1}}(G_{l-1}f_l)}{\eta_{l-1}^{P_{l-1}}(G_{l-1})} - \eta_{l-1}^{P_{l-1}}(f_{l-1}) \right\} + \frac{\eta_0^{P_0}(G_0f_1)}{\eta_0^{P_0}(G_0)}. \quad (3.6)$$

3.2 Mathematical Result

We consider the convergence of (3.6) in the case $m = 1$; this latter constraint can easily be removed with only minor changes to the subsequent notations and arguments. The analysis of Algorithm 1 has been considered in [5, 6]. However, there are some nuances that need to be adapted for the context under study. Throughout, we will suppose that for each $l \in \{2, 3, \dots\}$ we have chosen q_l so that for each $\theta_l \in \Theta_l$

$$\bar{\pi}_l(\theta_l) = \bar{\pi}_{l-1}(\theta_{l-1})q_l(\tilde{\theta}_l|\theta_{l-1}).$$

This means that

$$G_{l-1}(u_{l-1}) = \frac{p_l(y_{1:N}|\theta_l)}{p_{l-1}(y_{1:N}|\theta_{l-1})}.$$

This convention is not entirely necessary, but it will facilitate a simplification of the resulting calculations. We will use the following assumptions, which are often used in the analysis of approaches of the type described in Algorithm 1. Below \mathcal{E}_l is the Borel σ -field associated to \mathbf{E}_l .

(A1) 1. There exists a $0 < \underline{C} < \bar{C} < +\infty$ such that for any $x \in \mathbf{X}$:

$$\begin{aligned} \inf_{l \in \mathbb{N}} \inf_{u_{l-1} \in \mathbf{E}_{l-1}} \min\{p_l(y_{1:N}|u_{l-1}), \bar{\pi}_l(u_{l-1})\} &\geq \underline{C} \\ \sup_{l \in \mathbb{N}} \sup_{u_{l-1} \in \mathbf{E}_{l-1}} \max\{p_l(y_{1:N}|u_{l-1}), \bar{\pi}_l(u_{l-1}), f_l(x, u_{l-1})\} &\leq \bar{C}. \end{aligned}$$

2. There exists a $\rho \in (0, 1)$ such that for any $(l, u_{l-1}, u'_{l-1}, B_l) \in \mathbb{N} \times \mathbf{E}_{l-1}^2 \times \mathcal{E}_l$:

$$\int_{A_l} M_l(u_{l-1}, du_l) \geq \rho \int_{B_l} M_l(u'_{l-1}, du_l).$$

3. There exists a $C < \infty$ such that for any $(l, x) \in \{2, 3, \dots\} \times \mathsf{X}$:

$$\int_{\mathbf{E}_{l-1}} (f_l(x, u_{l-1}) - f_{l-1}(x, u_{l-2}))^2 \bar{\pi}_l(u_{l-1}) du_{l-1} \leq C n_l^{-\beta},$$

with the notation $u_{l-1} = (u_{l-2}, \tilde{\theta}_l)$.

4. There exists a $C < \infty$ and $\beta > 0$ such that for any $(l, u_{l-1}, x) \in \{2, 3, \dots\} \times \mathbf{E}_{l-1} \times \mathsf{X}$, $u_{l-1} = (u_{l-2}, \tilde{\theta}_l)$:

$$|p_l(y_{1:N}|u_{l-1}) - p_{l-1}(y_{1:N}|u_{l-2})| \leq C |f_l(x, u_{l-1}) - f_{l-1}(x, u_{l-2})|,$$

5. There exists a $r \geq 3$, $C < \infty$, possibly depending on r , such that for $\beta > 0$ as in 3. and any $(l, u, x) \in \{2, 3, \dots\} \times \mathbf{E}_{l-2} \times \mathsf{X}$:

$$\left(\int_{\mathbf{E}_{l-1}} |f_l(x, u_{l-1}) - f_{l-1}(x, u_{l-2})|^r M_{l-1}(u, du_{l-1}) \right)^{1/r} \leq C n_l^{-\beta/2},$$

with the notation $u_{l-1} = (u_{l-2}, \tilde{\theta}_l)$.

Admittedly, the minimum bound in A1.1 is not satisfied for most applications but does significantly simplify the proof. An approach similar to [5] can be used to relaxed this assumption. We then have the following result, whose proof is in Appendix A.

Proposition 3.1. *Assume (A1). Then there exists a $C < \infty$ and $\zeta \in (0, 1)$ such that for any $L \in \{2, 3, \dots\}$*

$$\mathbb{E}[(\hat{\pi}_L(f_L) - \pi_L(f_L))^2] \leq C \left(\frac{1}{P_0} + \sum_{l=2}^L \frac{1}{P_{l-1} n_l^\beta} + \sum_{2 \leq l < q \leq L} \frac{1}{(n_l n_q)^{\beta/2}} \left\{ \frac{\zeta^{q-1}}{P_{l-1}} + \frac{1}{P_{l-1}^{1/2} P_{q-1}} \right\} \right).$$

4 Trace class priors

In this section we briefly discuss our trace class priors, which we aim to analyze and motivate for numerical experiments later within the manuscript. We will begin with a formal definition, before providing a result related to convergence of the predictive model f . Given the rate obtained, we will then verify this rate through the demonstration of a simple numerical experiment.

The neural network priors we consider are the trace class neural networks, first proposed by Sell et al. [43]. These priors were introduced to mimic Gaussian priors $\bar{\pi}_0 \sim \mathcal{N}(0, \mathcal{C})$, for function-space inverse problems, where a common way to simulate Gaussian random fields is to use the Karhunen-Loève expansion

$$u = \sum_{j \in \mathbb{Z}^+} \sqrt{\lambda_j} \xi_j \Phi_j, \quad \xi_j \sim \mathcal{N}(0, I), \quad (4.1)$$

where $(\lambda_j, \Phi_j)_{j \in \mathbb{Z}^+}$ are the associated eigenbasis of the covariance function \mathcal{C} , and $\{\xi_j\}_{j \in \mathbb{Z}^+}$ is Gaussian white noise. For a detail description of the derivation and its application to stochastic numerical problems. we refer the reader to [41]. An issue that can arise with using (4.1) is that using such priors do not scale well with high-dimensional problems. This acts as the initial motivation for trace-class neural network (TNN) priors, where the work of Sell et al. [43] provided a justification for such priors. Specifically if one considers an infinite width network $n_l = \infty$, then the variances can be summarized in a diagonal covariance operator \mathcal{C} . Such a result is presented as [Theorem 1., [43]]. If we consider the TNN prior for $\theta_l := ((A_1^l, b_1^l), \dots, (A_D^l, b_D^l))$, then for $d = 1, \dots, D$, the associated weights and bias are defined as

$$A_{ij,d}^l \sim \mathcal{N}(0, (ij)^{-\alpha}), \quad b_{i,d}^l \sim \mathcal{N}(0, i^{-\alpha}), \quad (4.2)$$

where at level l a coupling can be constructed by letting $A_{ij,d}^l = A_{ij,d}^{l-1}$ and $b_{i,d}^l = b_{i,d}^{l-1}$ for $i, j \in \{1, \dots, n_{l-1}\}$ and $d \in \{2, D-1\}$; a similar assignment between layers l and $l-1$ is to be adopted for (A_1^l, b_1^l) and (A_D^l, b_D^l) . The notation A_i, b_i , for $i = 1, \dots, D$, θ , and σ , will be used to denote the limits $\lim_{l \rightarrow \infty} A_i^l, b_i^l, \theta^l, \sigma_{n_l}$. Then our limiting TNN prior replaces (4.1) with $u = f$, the notation in Section 2 and (2.4) (except for $n_l = 2^l$) and above in (4.2), for $d = 2, \dots, D$

$$g_d(x, \theta) = A_d \sigma(g_{d-1}(x)) + b_d. \quad (4.3)$$

The approximation at level l , f_l , simply replaces all limiting objects with the level l approximations (with width $n_l = 2^l$ for all hidden layers). The tuning parameter α controls how much information one believes concentrates on the first nodes. In the case of $\alpha > 1$, we refer to the prior as trace-class, which results in the term trace-class neural network prior.

As we are concerned with combining such priors to the MLSMC sampler, it would be of interest to analyze the convergence of such neural networks which use (4.2). Therefore we provide a result establishing Assumption 3, in terms of the parameters l and α , which is given through the following proposition.

Proposition 4.1. *Assume that for all $z \in \mathbb{R}$, $\sigma(z) \leq |z|$. Then for $\alpha > 1/2$, the priors defined as in (4.2) are trace-class. Furthermore, let $x \in \mathbf{X}$, and consider the TNN $f_l(x, \theta_l)$ truncated at $n_l = 2^l$ terms, for $l \in \mathbb{N}$, with the limit denoted $f(x, \theta) = \lim_{l \rightarrow \infty} f_l(x, \theta_l)$, as described above. Then there is a $C(x) < +\infty$ such that*

$$\mathbb{E}|f_l(x, \theta_l) - f(x, \theta)|^2 \leq C 2^{-(2\alpha-1)l}. \quad (4.4)$$

Proof. First assume that $D = 2$, i.e. there is a single hidden layer, and $m = 1$. Let $x \in \mathbf{X}$ be fixed, but allow the possibility that $n \rightarrow \infty$, provided that $\sum_j |x_j|^2 < \infty$ almost surely.

Let $A_{k,1}^l$ denote the k^{th} row of A_1^l , allowing the possibility that $l \rightarrow \infty$ (denoted simply A_1 , as described above), and observe that

$$\mathbb{E}(A_{k,1}^l x + b_{k,1}^l) = 0, \quad \mathbb{E}((A_{k,1}^l x + b_{k,1}^l)^2) = k^{-\alpha} \left(\sum_{j=1}^n j^{-\alpha} x_j^2 + 1 \right) \leq k^{-\alpha} (|x|^2 + 1), \quad (4.5)$$

where $|x|^2 := \sum_{j=1}^n x_j^2$.

Let $A_{k,2}^l$ denote the k^{th} entry of the vector $A_2^l \in \mathbb{R}^{n_l}$, again allowing $l \rightarrow \infty$ (and denote the limit by A_2). Using the shorthand notation $\xi_{k,1}^l = A_{k,1}^l x + b_{k,1}^l$ (and $\xi_{k,1} = A_{k,1} x + b_{k,1}$), we are concerned with

$$\begin{aligned} \mathbb{E}f^2(x, \theta) &= \sum_{k=1}^{\infty} \mathbb{E}(A_{k,2})^2 \mathbb{E}\sigma(\xi_{k,1})^2 + \mathbb{E}(b_2)^2 \\ &\leq \sum_{k=1}^{\infty} \mathbb{E}(A_{k,2})^2 \mathbb{E}(\xi_{k,1})^2 + 1 \\ &\leq C \sum_{k=1}^{\infty} k^{-2\alpha} + 1. \end{aligned} \quad (4.6)$$

This shows that the output has finite second moment for $\alpha > 1/2$. Furthermore, a simple extension of the above calculation shows that the rate of convergence is given by

$$\mathbb{E}|f_l(x, \theta_l) - f(x, \theta)|^2 \leq C \sum_{k \geq 2^l} k^{-2\alpha} \leq C 2^{-(2\alpha-1)l}.$$

Now, regarding multiple levels, we can proceed by induction. Assume we have (4.6) at level d , with $\xi_d^l \in \mathbb{R}^{n_l}$ denoting the output at level d (e.g. $\xi_{m,2}$ replaces f in (4.6), for $m = 1, \dots$). As above, let $A_{k,d+1}^l$ denote the k^{th} row of the matrix A_{d+1}^l . Then, by iterating expectations, we have a $C < +\infty$ such that

$$\mathbb{E}((A_{k,d+1}^l \xi_d^l + b_{k,d+1}^l)^2) \leq C k^{-\alpha},$$

as in (4.5). This brings us back to (4.6) at level $d+1$, and we are done for $D > 2$. \square

The result above establishes Assumption (A1.3) for $\beta = 2\alpha - 1$. It also provides (A1.5) for $r = 2$ when combined with (A1.1), (A1.2) and the definition (3.2).

4.1 Numerical Result

To verify the rate which was obtained in Proposition 4.1, we provide a simple numerical example which analyzes (4.4), in the context of our trace class priors. For our experiment we consider a setup of $\alpha = 2$, implying that our decay rate is $\beta = 2\alpha - 1 = 3$. We test this on both a 2 layer and 3 layer NN, and with a ReLU activation function $\sigma(z) = \max\{z, 0\}$, and $\sigma(z) = \tanh(z)$ activation function. Our experiment is presented in Figures 1 - 2.

We observe that in both figures, as a result of using TNN priors, our decay rate matches that of (4.4), where we obtain the canonical rate of convergence. As a side example, to show that this is not attained with other choices, we compare this other choices of priors. This can be seen from Figure 2, where we notice that the rates are not as expected, implying that they are sub-canonical. Therefore this provides a motivation in using trace class NN priors, coupled with MLMC, which we exploit in the succeeding subsection.

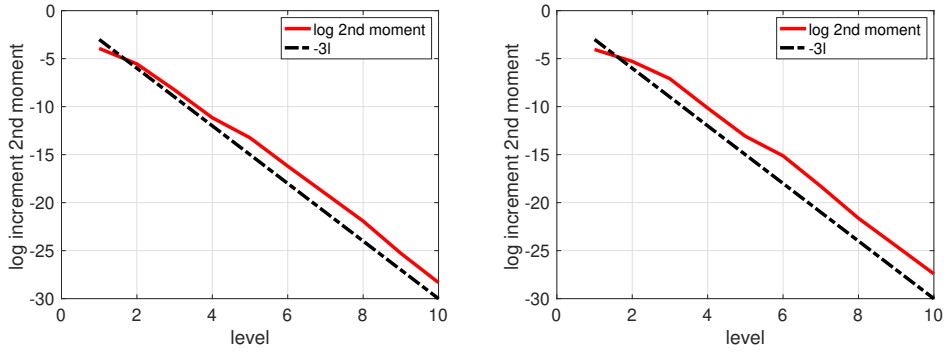


Figure 1: Increment 2nd moment vs. levels. The decay is $\mathcal{O}(2^{-3l})$ with levels for a 3 layer neural network. Therefore the variance decays faster than $1/\text{cost}$, which is the canonical regime. Left: activation function of $\text{ReLU}(z) = \max\{0, z\}$. Right: activation function of $\sigma(z) = \tanh(z)$.

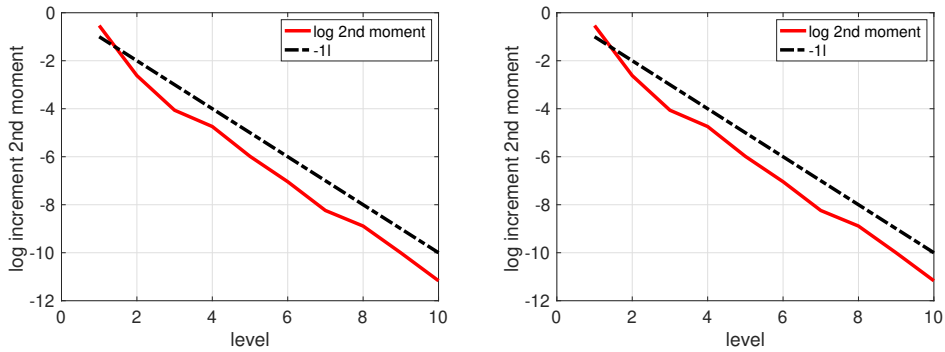


Figure 2: Increment 2nd moment vs. levels. The decay is $\mathcal{O}(2^{-l})$ with levels for 2 layer neural network. Therefore the variance decays slower than $1/\text{cost}$, which is a sub-canonical regime. Left: activation function of $\text{ReLU}(z) = \max\{0, z\}$. Right: activation function of $\sigma(z) = \tanh(z)$.

5 Numerical Experiments

For this section we provide our main numerical experiments, which is to use our TNN priors on various Bayesian tasks related to machine learning. Specifically we will aim to use these priors with the proposed methodology of Algorithm 1, comparing it to single-level Monte Carlo SMC sampler which use the same priors. We will test this on a range of machine learning tasks, which include regression, classification and reinforcement learning, where we hope to show the benefit of using MLMC, by attaining the canonical rate of convergence.

5.1 Regression Problem

Our first numerical experiment will be based on a Bayesian regression problem given in (2.1). Our objective is to identify the posterior distribution on θ specified in (2.4) with the likelihood specified in (2.5)

$$\pi(\theta|y_{1:N}) \propto p(y_{1:N}|\theta, x_{1:N})\bar{\pi}(\theta), \quad p(y_{1:N}|\theta, x_{1:N}) = \prod_{i=1}^N \phi_m(y_i; f(x_i, \theta), \Sigma_i),$$

where $\bar{\pi}(\theta)$ is the TNN prior (4.2), discussed in Section 4. This can subsequently be used for prediction at a new test data point x^*

$$\mathbb{E}(f(x^*)|\mathcal{D}) = \int_{\Theta} f(x^*, \theta)\pi(\theta|\mathcal{D})d\theta,$$

as well as for the computation of other posterior predictive quantities such as the variance

$$\mathbb{V}(f(x^*)|\mathcal{D}) = \int_{\Theta} (f(x^*, \theta) - \mathbb{E}(f(x^*)|\mathcal{D}))^2\pi(\theta|\mathcal{D})d\theta,$$

For our observational noise we take $\Sigma_i^2 = 0.01^2 I$. We use a TNN prior with a tanh activation function, i.e. $\sigma(z) = \tanh(z)$. We take $n_l = 2^l$ for $l = 7$ for our reference solution. For this model we specify $N = 200$, and consider $X = \mathbb{R}^{10}$ so the input NN width is $n_0 = 10$, and the data points are generated as normal distributed random variables, i.e. $x_i (\in \mathbb{R}^{10}) \sim \mathcal{N}(2, 0.5)$. Then for each x_i , the following model produces y_i . To compute the MSE we consider 100 replications, and then take the MSE. We will compare and apply an SMC sampler and multilevel counterpart, i.e. a MLSMC sampler. The setup of the MLSMC sampler is presented in Algorithm 1. In this first experiment we will apply both these methodologies and observe the error-to-cost rate ξ such that $\text{cost} \propto \text{MSE}^{-\xi}$. We will compare this for different values of $\beta = 2\alpha - 1$. Recall that the $\text{cost} = \mathcal{O}(2^{\gamma l})$, with $\gamma = 2$, so as a rule of thumb one should expect the attain a canonical rate of convergence when $\alpha > 1.5$ and $\beta > \gamma$.

Below in Figure 3 we present some preliminary results of applying both SMC sampler and a MLSMC sampler. As mentioned, further details on the MLSMC sampler can be found in [6]. We conduct our numerical experiment with levels $L \in \{3, 4, \dots, 7\}$. The first numerical results are presented in Figure 3 which compares values of $\alpha = \{1.7, 1.9, 2, 3\}$. We plot both the SMC sampler and MLSMC sampler where the prior for each method is our TNN prior. Furthermore we also plot the credible sets around the MSE values, given by the thin blue and red curves.

As we can observe from the results, in general applying MLMC shows benefits were as the MSE becomes smaller, the gap between both methods becomes larger related to the computational cost. We can see that the difference in cost for the lowest MSE is approximately a factor of 10. This indicates that the error-to-cost rates are different, and to verify our theoretical findings we plot the canonical rate in black, which matches that of our proposed methodology. The results thus far are for values of α which attain the canonical rate. Now let us consider alternative choices of α , which should result in a sub-canonical rate.

5.1.1 Sub-canonical rates

Let us now consider the same experiments but where we modify the parameter values of $\alpha \leq 1.5$. In this case, $\beta \leq \gamma = 2$, where the cost of a single simulation of f_l is $\mathcal{O}(2^{\gamma l})$, so sub-canonical convergence is

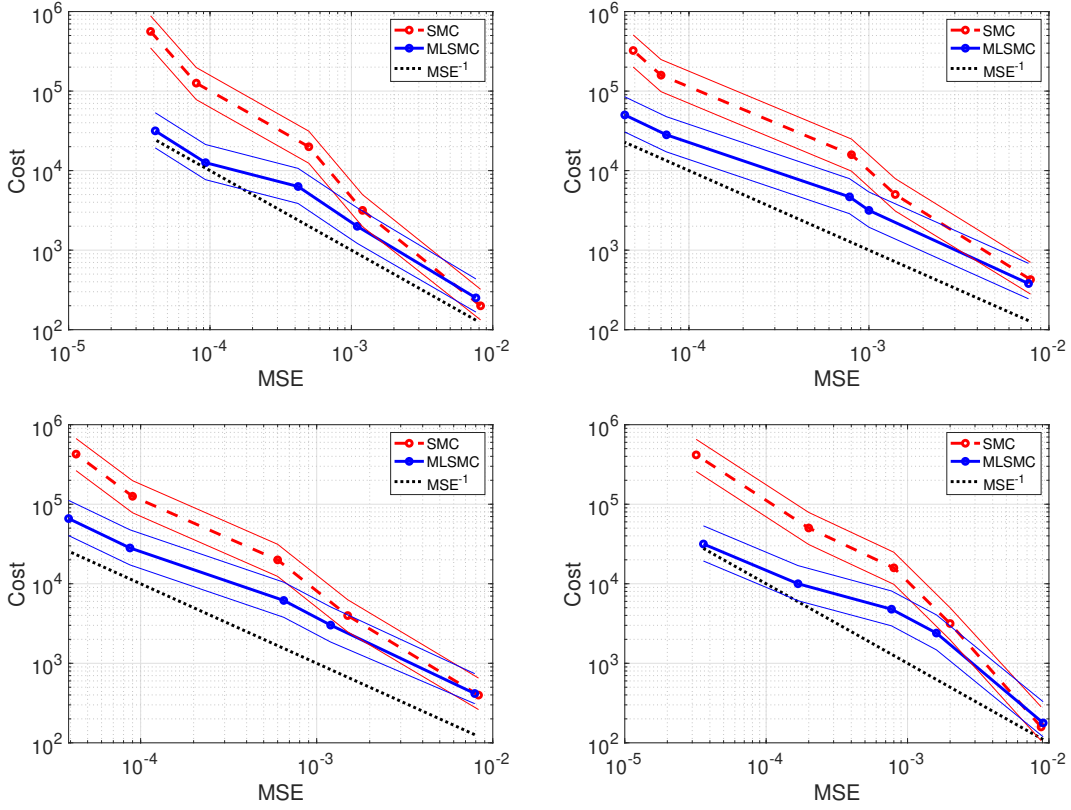


Figure 3: Regression problem: error vs cost plots for SMC and MLSMC using TNN priors. Top left: $\alpha = 3$. Top right: $\alpha = 2.0$. Bottom left: $\alpha = 1.9$. Bottom right: $\alpha = 1.7$. Credible sets are provided in the thin blue and red curves.

expected. We will consider two choices of $\alpha \in \{1.1, 1.4\}$, where we keep the experiment and the parameter choices the same. Our results are presented in Figure 4. As expected, the complexity rate is closer to the single level case, but an improvement factor of around 3 is still observed at the resolutions considered.

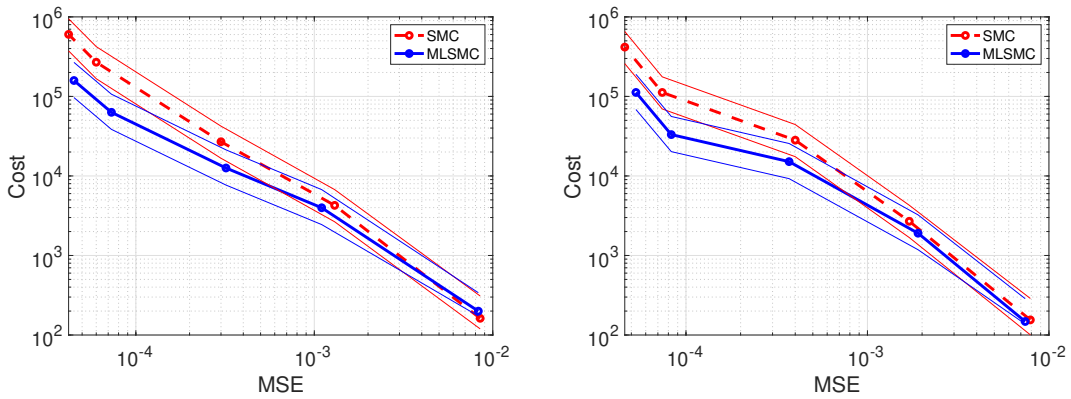


Figure 4: Regression problem: error vs cost plots for SMC and MLSMC using TNN priors. Left: $\alpha = 1.4$. Right: $\alpha = 1.1$. Credible sets are provided by thin blue and red curves.

The results from Figure 4 indicate that if we consider TNN priors of lower regularity, then we can expect to achieve sub-canonical rates, in the complexity related to the MSE-to-cost ratio. This promotes the question, of whether canonical rates, in our setup & framework are possible for non-smooth random fields. This, and related questions, will be considered for future work.

5.2 Classification Problem

Following the definition of the classification model (2.2), just as we considered the likelihood (2.5) for the regression problem, we consider the likelihood (2.6) for the classification problem. The posterior is again given by (2.4). Again predictions at an input $x^* \notin \mathcal{D}$ are delivered by the posterior predictive distribution. For example, the marginal posterior class probability $\mathbb{P}(k|x^*, \mathcal{D})$ is given by

$$\mathbb{P}(k|x^*, \mathcal{D}) = \int_{\Theta} h_k(x^*, \theta) p(\theta|\mathcal{D}) d\theta,$$

and the variance associated to a prediction of class k for input x^* is given by

$$\mathbb{V}(k|x^*, \mathcal{D}) = \int_{\Theta} h_k(x^*, \theta)^2 p(\theta|\mathcal{D}) d\theta - \mathbb{P}(k|x^*, \mathcal{D})^2.$$

For our classification problem we are interested in classifying two data sets, where the data is based on a 2D spiral. In other words, the data for class $k = 1$ is generated through the following equations, for $i = 1, \dots, N = 500$

$$\begin{aligned} x_{i1} &= av_i^p \cos(2t_i^p \pi) + \epsilon_{i1}, \\ x_{i2} &= av_i^p \sin(2t_i^p \pi) + \epsilon_{i2}, \end{aligned}$$

where $v_i, t_i \sim \mathcal{U}[0, 1]$ uniform, $\epsilon_i \sim \mathcal{N}(0, 0.1^2)$ and the parameter choices are $a = 16$ and $p = 0.05$. The data associated to class $k = 2$ is generated similarly, except with a shift of π in the arguments of the trigonometric functions. This data can be seen in Figure 5, where our two classes correspond to the colors, i.e. data labelled as Class $k = 1$ is blue and data labelled as Class $k = 2$ is yellow. The setup for the classification problem is similar to the regression problem. Again we conduct experiments for different choices of α , i.e. $\alpha = \{1.7, 1.9, 2, 3\}$ and levels $L \in \{3, 4, \dots, 7\}$. Our parameter choices are the same as the regression problem. For our reference solution we again use $n_7 = 2^7$ with a *tanh* activation function, for the prior and take a high-resolution solution. We present firstly in Figure 6 the results related to the canonical rates obtained for the MSE-to-cost rates. As we observe, we see a clear distinction in the difference in costs as the MSE is decreased, with again roughly a magnitude of $\sim \mathcal{O}(10^1)$. This again highlights the computationally efficiency of our proposed methodology, with the combination of our TNN prior. For our final experiments for the classification problem, we consider alternative values of α , i.e., $\alpha \in \{1.1, 1.4\}$, which are presented in Figure 7. Again, similar to the regression problem, we observe that sub-canonical rates are obtained for $\alpha < 1.5$, where the difference in cost for the lower value of MSEs is not as significant.

5.3 Reinforcement Learning

5.3.1 Setup

Our final numerical example will consist of an inverse reinforcement learning problem [42, 46]. Unlike the previous two examples, reinforcement learning is not concerned with pattern formations, but instead decision making. Specifically it is used to solve stochastic optimal control problems. Before we continue with the specific example, we first recall some common notation and provide our setup for Bayesian reinforcement learning, which is largely motivated and taken from [43].

A Markov decision process is defined by a controlled Markov chain $\{X_t\}_{t \in \mathbb{N}}$, referred to as the state process, the control process $\{A_t\}_{t \in \mathbb{N}}$ and the an optimality criterion. The state process takes values in a

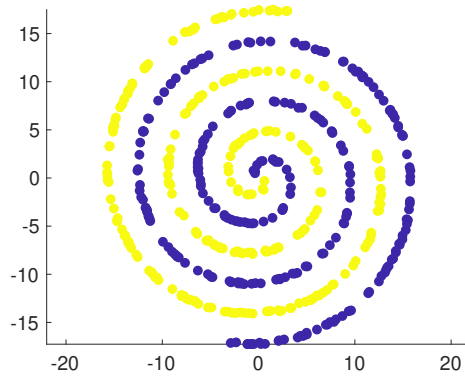


Figure 5: Classification problem: Our data is generated as a 2D spiral with two classes, Class $k = 1$ being in blue and Class $k = 2$ in yellow.

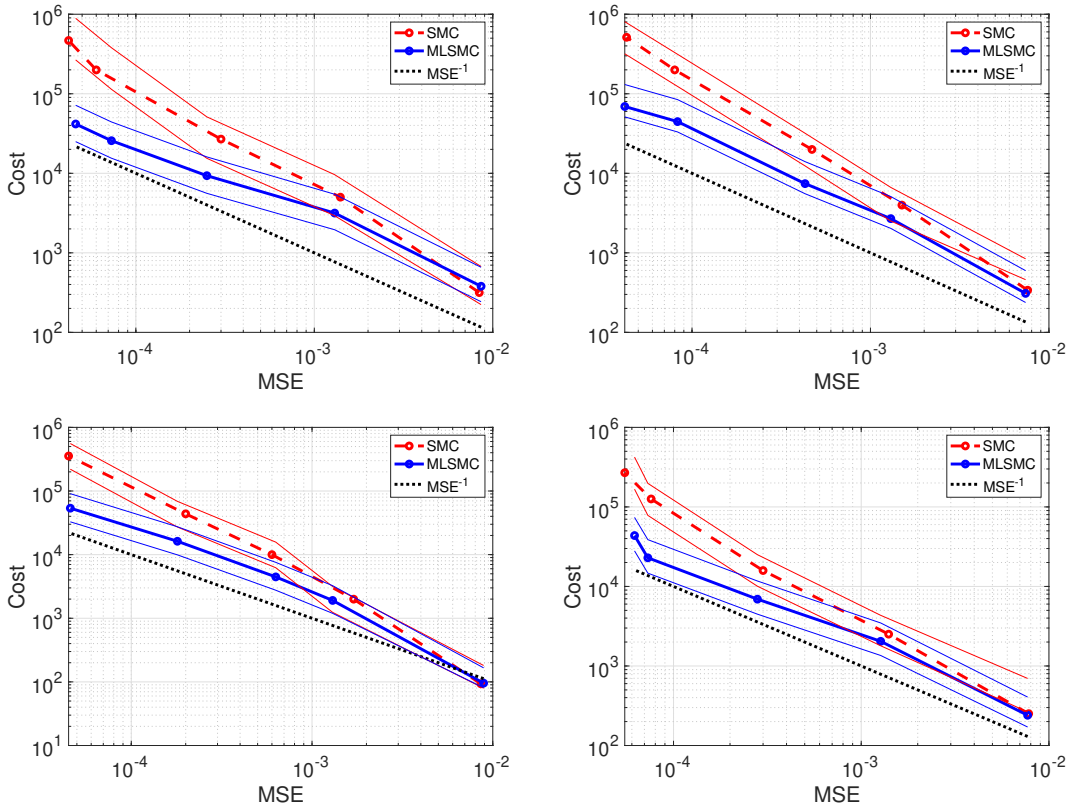


Figure 6: Classification problem: error vs cost plots for SMC and MLSMC, using TNN priors. Top left: $\alpha = 3$. Top right: $\alpha = 2.0$. Bottom left: $\alpha = 1.9$. Bottom right: $\alpha = 1.7$. Credible sets are provided in the thin blue and red curves.

bounded set $\mathcal{X} \subset \mathbb{R}^d$. The control process is \mathcal{A} -valued with $\mathcal{A} = \{1, \dots, M\}$. Therefore the state process propagates by

$$X_{t+1} | (X_{1:t} = x_{1:t}, A_{1:t} = a_{1:t}) \sim p(\cdot | x_t, a_t),$$

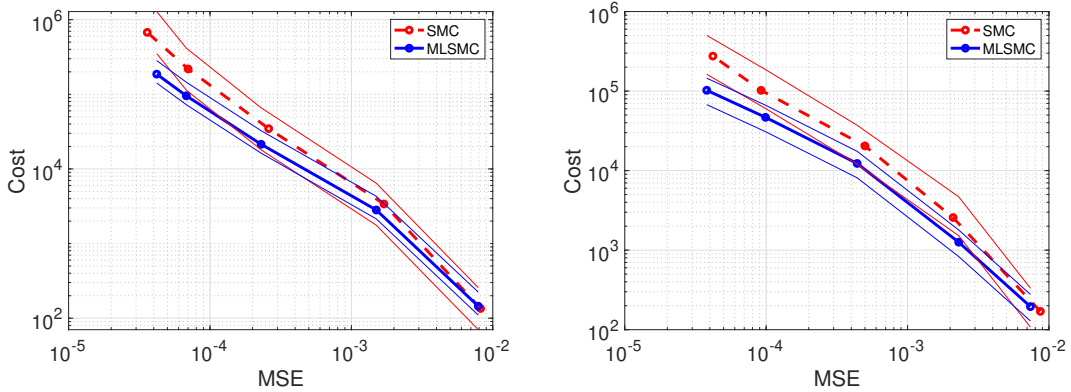


Figure 7: Classification problem: error vs cost plots for SMC and MLSMC, using TNN priors. Left: $\alpha = 1.4$. Right: $\alpha = 1.1$. Credible sets are provided in the thin blue and red curves.

where for any state-action pair (x_t, a_t) , $p(\cdot|x_t, a_t)$ is a probability density. Now let $r : \mathcal{X} \rightarrow \mathbb{R}$ be the reward function, then the accumulated reward given in a policy and initial state $X_1 = x_1$ is

$$C_\mu(x_1) = \mathbb{E}_\mu \left[\sum_{t=1}^{\infty} \beta^t r(X_t) | X_1 = x_1 \right],$$

where $\beta \in (0, 1)$ is a discount factor and $\mu : \mathcal{X} \rightarrow \mathbb{R}$ is the policy mapping. A policy μ^* is optimal if $C_{\mu^*}(x_1) > C_\mu(x_1)$, for all $(\mu, x_1) \in \mathcal{X} \times \mathbb{R}$, and can be found by solving Bellman's fixed point equation [4]. Using this fixed point solution $v : \mathcal{X} \rightarrow \mathbb{R}$, we can derive the optimal policy by

$$\mu^*(x) = \arg \max_{a \in \mathcal{A}} \left[\int_{\mathcal{X}} p(x'|x, a) v(x') dx' \right], \quad (5.1)$$

that is, the optimal action at any state is the one that maximizes the expected value function at the next state. It is assumed that the state evolution is deterministic, i.e., there is a map $\mathcal{T} : \mathcal{X} \times \mathcal{A} \rightarrow \mathcal{X}$ such that $p(x'|x, a) = \delta_{\mathcal{T}(x, a)}(x')$. Noise is added to model imperfect action selections so that at each time step the chosen action is a random variable given by

$$A_t(x_t) = \arg \max_{a \in \mathcal{A}} \left[v(\mathcal{T}(x_t, a)) + \epsilon_t(a) \right], \quad \epsilon_t \sim \mathcal{N}(0, \sigma^2 I). \quad (5.2)$$

Now what remains is to define our likelihood function associated to our example. Our data will consist of a collection of noise corrupted state-action pairs $\{x_t, a_t\}_{t=1}^T$, and the aim is to infer the value function (5.1) that leads to the actions a_t for the current state x_t . Using the noisy action selection process (5.2) we have the likelihood function defined as

$$\mathcal{L}(a_{1:T} | x_{1:T}, v, \sigma) = \prod_{t=1}^T p(a_t | x_t, v, \sigma) = \prod_{t=1}^T p(a_t | v_t, \sigma), \quad (5.3)$$

where $v_t \in \mathbb{R}^M$ is defined by $v_{t,k} = v(\mathcal{T}(x_t, a = k))$. Following from (5.2), the factors in (5.3) have a closed form expression

$$p(a_t | v_t, \sigma) = \frac{1}{\sigma} \int_{\mathbb{R}} \phi \left(\frac{t - v_{t, a_t}}{\sigma} \right) \prod_{\substack{i=1 \\ i \neq a_t}}^M \Phi \left(\frac{t - v_{t, i}}{\sigma} \right) dt,$$

where ϕ and Φ denote the standard normal PDF and CDF, respectively. The derivation can be found in [43].

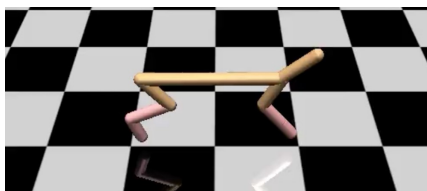


Figure 8: Plot of HalfCheetah, which has states $x_t \in \mathbb{R}^{17}$. Its goal is to run as quickly as possible, while not moving its body parts more than necessary.

5.3.2 Experiment

For our Bayesian reinforcement learning example, we consider the HalfCheetah example [45], where the goal is for the HalfCheetah to run as fast as possible without moving its body more than necessary. The state space is $\mathcal{X} = \mathbb{R}^{17}$, and the action space is $\mathcal{A} = \{1, \dots, 8\}$. We also take $T = 100$ for the observations, where the data generation is taken similarly to [43], and $\sigma^2 = 0.01^2$. As before we aim to show the benefit of MLMC for the SMC sampler, where we choose values $\alpha = \{1.7, 1.9, 2, 3\}$ with levels $L \in \{3, 4, \dots, 7\}$. For our truth we again take a high-resolution solution to our problem, similarly to what was done for the 2D spiral experiment. These values are again chosen such that we can attain the canonical rate of convergence. Our results are presented in Figure 9 which compare both methodologies with TNN priors, for the different values of α . Similarly to our previous results we notice a bigger difference is cost for lower values of the MSE, which indicate both error-to-cost rates are different. As done for the previous experiments, we plot the canonical rate in black to verify our methodology attains the rate.

Finally our last experiment is to verify that one cannot attain the canonical rate if we assume that $\alpha < 1.5$. In Figure 10 we present similar experiments to Figure 9, but with modified values of $\alpha \in \{1.1, 1.4\}$. We can observe that the results are similar to the previously attained, in the sense that the complexity grows at a faster rate than it does in the canonical case, but still slower than for the single level approach. Again this verifies the theory.

6 Conclusion

The development of machine learning methodologies is of high relevance now, due to the availability of data and modern advanced algorithms. In this work we considered the application of multilevel Monte Carlo (MLMC) for various Bayesian machine learning problems, where we exploited the use of trace-class neural network (TNN) priors. These flexible priors scale gracefully to high input dimensions, and have been previously used on a range of Bayesian inference tasks. In the present work, we combine TNN priors with the powerful multilevel sequential Monte Carlo (MLSMC) sampler algorithm, which is designed around the MLMC framework. In particular, we prove that one attains strong convergence, unlike other priors based on neural network methodologies, and hence also a bound on mean square error (MSE). Within the MLMC framework described above, this reduces the complexity in terms of MSE, and often to the canonical $\text{Cost} \propto 1/\text{MSE}$ rate. Numerical experiments were conducted on a range of common machine learning problems, which includes regression, classification and reinforcement learning, where we were able to verify the reduction in computational cost to achieve a particular order of MSE.

For future considerations of work, one natural direction is to see if one can extend this work to multi-index Monte Carlo [23], which has shown to gain efficiency over MLMC methods. Another direction is to consider other applications beyond this work, such as clustering. In a Bayesian context, such popular methods would be the likes of Bayesian hierarchical clustering [21, 29] which is related to mixture models. One could also exploit more advanced Monte Carlo proposals, based on gradient information, which could enhance the performance – for example, Metropolis adjusted Langevin algorithm, Hamiltonian Monte Carlo, or more sophisticated versions thereof. These examples, and others, will be considered in future work. As eluded to in the numerical experiments, one could consider alternative forms of TNN priors.

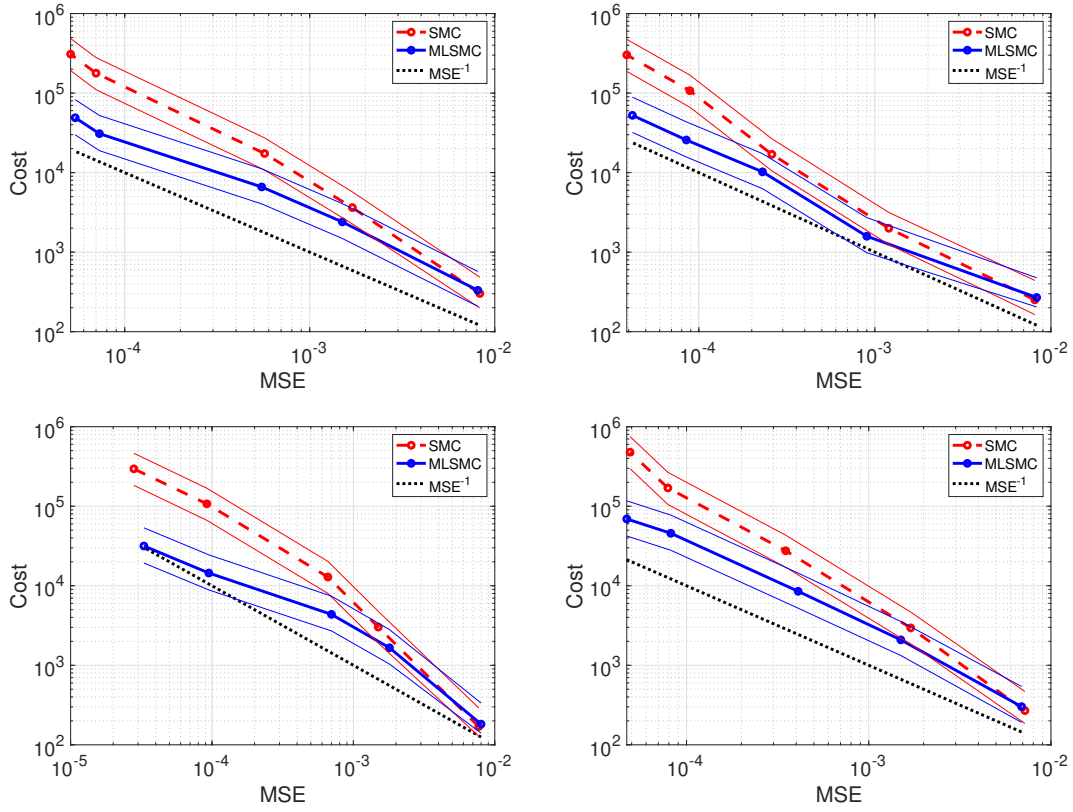


Figure 9: Reinforcement learning: error vs cost plots for SMC and MLSMC, using TNN priors. Top left: $\alpha = 3$. Top right: $\alpha = 2.0$. Bottom left: $\alpha = 1.9$. Bottom right: $\alpha = 1.7$. Credible sets are provided in the thin blue and red curves.

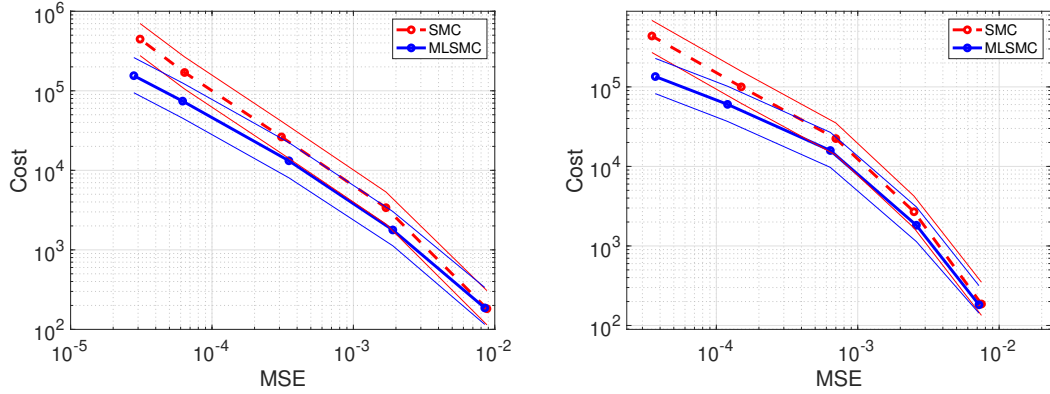


Figure 10: Reinforcement learning: error vs cost plots for SMC and MLSMC, using TNN priors. Left: $\alpha = 1.4$. Right: $\alpha = 1.1$. Credible sets are provided in the thin blue and red curves.

Acknowledgments

AJ and NKC are supported by KAUST baseline funding.

A Proofs for Proposition 3.1

The proof of Proposition 3.1 essentially follows that of [5, Theorem 3.1], except there are some modifications required. We mainly provide details of these additional calculations, but we remark that to fully understand the proof, one must have read [5]. We make the definition that $\eta_0 = q_0$ and that for any $l \in \{1, \dots, L-1\}$

$$\eta_l(du_l) = \frac{\int_{E_0 \times \dots \times E_{l-1}} \{\prod_{p=0}^{l-1} G_p(u_p)\} \eta_0(u_0) \prod_{p=1}^l M_p(u_{p-1}, du_p) du_0}{\int_{E_0 \times \dots \times E_l} \{\prod_{p=0}^{l-1} G_p(u_p)\} \eta_0(u_0) \prod_{p=1}^l M_p(u_{p-1}, du_p) du_0}.$$

Note that it easily shown that for any $l \in \{1, \dots, L\}$ and any measurable $\varphi_l : \Theta_l \rightarrow \mathbb{R}$ that is π_l -integrable that

$$\pi_l(\varphi_l) = \int_{E_l} \varphi(u_{l-1}) \eta_l(d(u_{l-1}, \tilde{\theta}_{l+1})),$$

where

$$\eta_l(d(u_{l-1}, \tilde{\theta}_{l+1})) = \pi_l(du_{l-1}) q_{l+1}(d\tilde{\theta}_{l+1} | u_{l-1}).$$

From herein C is a finite constant whose value may change on each appearance, but, does not depend upon l . We will also make use of the C_p inequality. For two real-valued random variables X and Y defined on the same probability space, with expectation operator \mathbb{E} , suppose that for some fixed $p \in (0, \infty)$, $\mathbb{E}[|X|^p]$ and $\mathbb{E}[|Y|^p]$ are finite, then the C_p -inequality is

$$\mathbb{E}[|X + Y|^p] \leq C_p \left(\mathbb{E}[|X|^p] + \mathbb{E}[|Y|^p] \right), \quad (\text{A.1})$$

where $C_p = 1$, if $p \in (0, 1)$ and $C_p = 2^{p-1}$ for $p \in [1, \infty)$.

Proof of Proposition 3.1. For any $l \in \{2, 3, \dots\}$, we have the decomposition

$$\frac{\eta_{l-1}^{P_{l-1}}(G_{l-1}f_l)}{\eta_{l-1}^{P_{l-1}}(G_{l-1})} - \eta_{l-1}^{P_{l-1}}(f_{l-1}) - \left\{ \frac{\eta_{l-1}(G_{l-1}f_l)}{\eta_{l-1}(G_{l-1})} - \eta_{l-1}(f_{l-1}) \right\} = \sum_{j=1}^3 T_j^{P_{l-1}},$$

where

$$\begin{aligned} T_1^{P_{l-1}} &= -\frac{\eta_{l-1}^{P_{l-1}}(G_{l-1}f_l)}{\eta_{l-1}^{P_{l-1}}(G_{l-1})} [\eta_{l-1}^{P_{l-1}} - \eta_{l-1}] \left(\frac{Z_l}{Z_{l-1}} G_{l-1} - 1 \right), \\ T_2^{P_{l-1}} &= [\eta_{l-1}^{P_{l-1}} - \eta_{l-1}] \left(f_l \left\{ \frac{Z_l}{Z_{l-1}} G_{l-1} - 1 \right\} \right), \\ T_3^{P_{l-1}} &= [\eta_{l-1}^{P_{l-1}} - \eta_{l-1}] (f_l - f_{l-1}), \end{aligned}$$

which makes use of (3.5) - (3.6), and the fact that

$$\frac{Z_l}{Z_{l-1}} G_{l-1} - 1 = \frac{Z_l}{Z_{l-1}} [G_{l-1} - 1] - \frac{Z_{l-1} - Z_l}{Z_{l-1}}.$$

As a result, by using the C_2 -inequality, from (A.1) we can consider

$$\mathbb{E}[(\hat{\pi}_L(f_L) - \pi_L(f_L))^2] \leq C \left(\mathbb{E} \left[\left(\frac{\eta_0^{P_0}(G_0 f_1)}{\eta_0^{P_0}(G_0)} - \frac{\eta_0(G_0 f_1)}{\eta_0(G_0)} \right)^2 \right] + \sum_{j=1}^3 \mathbb{E} \left[\left(\sum_{l=2}^L T_j^{P_{l-1}} \right)^2 \right] \right), \quad (\text{A.2})$$

where C does not depend upon l . For the first-term on the R.H.S. of (A.2) by standard results (see e.g. [5, Lemma A.3.]) we have

$$\mathbb{E} \left[\left(\frac{\eta_0^{P_0}(G_0 f_1)}{\eta_0^{P_0}(G_0)} - \frac{\eta_0(G_0 f_1)}{\eta_0(G_0)} \right)^2 \right] \leq \frac{C}{P_0}.$$

For the summands on the R.H.S. of (A.2) we can apply Remark A.1 to conclude the proof. \square

To give our technical results, we require some notations. To connect with the appendix in [5], we use the same subscript conventions (i.e. n, p instead of l). Let $p \in \mathbb{N} \cup \{0\} = \mathbb{N}_0$ then $Q_{p+1}(u, dv) = G_p(u)M_{p+1}(u, dv)$ and for $0 \leq p \leq n \in \mathbb{N}_0$ we set for $u_p \in \mathbb{E}_p$ and $\varphi : \mathbb{E}_n \rightarrow \mathbb{R}$ bounded and measurable (write the collection of such functions as $\mathcal{B}_b(\mathbb{E}_n)$)

$$Q_{p,n}(\varphi)(u_p) := \int_{\mathbb{E}_{p+1} \times \dots \times \mathbb{E}_n} \varphi(u_n) \prod_{q=p+1}^n Q_q(u_{q-1}, du_q),$$

with $Q_{n,n}$ the identity operator. Then for $(u_p, \varphi_n) \in \mathbb{E}_p \times \mathcal{B}_b(\mathbb{E}_n)$ set

$$D_{p,n}(\varphi_n)(u_p) = \frac{Q_{p,n}(\varphi_n - \eta_n(\varphi_n))(u_p)}{\eta_p(Q_{p,n}(1))},$$

with $D_{n,n}(\varphi_n)(u_n) = \varphi_n - \eta_n(\varphi_n)$. Then we make the definitions, with μ a probability measure on \mathbb{E}_p , $(\varphi_p, \varphi_n) \in \mathcal{B}_b(\mathbb{E}_p) \times \mathcal{B}_b(\mathbb{E}_n)$

$$\begin{aligned} \Phi_p(\mu)(\varphi) &= \frac{\mu(G_{p-1}M_p(\varphi_p))}{\mu(G_{p-1})}, \\ V_p^{P_p}(\varphi_p) &= \sqrt{P_p}[\eta_p^{P_p} - \Phi_p(\eta_{p-1}^{P_{p-1}})](\varphi_p), \\ R_{p+1}^{P_p}(D_{p,n}(\varphi_n)) &= \frac{\eta_p^{P_p}(D_{p,n}(\varphi_n))}{\eta_p^{P_p}(G_p)}[\eta_p - \eta_p^{P_p}](G_p). \end{aligned}$$

The following decomposition is then well-known (see [5, 11]) for $\varphi_n \in \mathcal{B}_b(\mathbb{E}_n)$

$$[\eta_n^{P_n} - \eta_n](\varphi_n) = \sum_{p=0}^n \frac{V_p^{P_p}(D_{p,n}(\varphi_p))}{\sqrt{P_p}} + \sum_{p=0}^{n-1} R_{p+1}^{P_p}(D_{p,n}(\varphi_n)).$$

Given the terms in (A.2) it is then necessary to deal with the decomposition above. This has largely been done in the proof of Theorem 3.1. in [5]. However, in order to use the proof there, one must provide an appropriate adaptation of [5, Lemma A.1. (i)-(iii)] and this is the subject of the following result. Below, for a scalar random variable Z , we use the notation $\|Z\|_r = \mathbb{E}[|Z|^r]^{1/r}$.

Lemma A.1. *Assume (A1). Then there exists a $C < \infty$, possibly depending upon r in (A1) 5., and $\zeta \in (0, 1)$ such that for any $0 \leq p \leq n$, $\varphi_n \in \left\{ f_{n+1} - f_n, \frac{Z_{n+1}}{Z_n}G_n - 1, f_{n+1} \left(\frac{Z_{n+1}}{Z_n}G_n - 1 \right) \right\}$ and β as in (A1) 3.)*

1. $\sup_{u_p \in \mathbb{E}_p} |D_{p,n}(\varphi_n)(u_p)| \leq C\zeta^{n-p}n_l^{-\beta/2}$, ($0 \leq p < n$).
2. $\|V_p(D_{p,n}(\varphi_n))\|_r \leq C\zeta^{n-p}n_l^{-\beta/2}$, (r as in (A1) 5.).
3. $\|R_{p+1}^{P_p}(D_{p,n}(\varphi_n))\|_r \leq C\zeta^{n-p}n_l^{-\beta/2}$, ($0 \leq p < n$, r as in (A1) 5.).

Proof. Throughout the proof, we only consider the case $\varphi_n = \frac{Z_{n+1}}{Z_n}G_n - 1$. The other cases can be dealt with in a similar manner. We start with 1. and noting that

$$\frac{Z_{n+1}}{Z_n}G_n - 1 = \frac{Z_{n+1}}{Z_n}(G_n - 1) + \frac{Z_{n+1}}{Z_n} - 1. \quad (\text{A.3})$$

Therefore

$$D_{p,n}(\varphi_n)(u_p) = \frac{Z_{n+1}}{Z_n}D_{p,n}(G_n - 1)(u_p) \leq C|D_{p,n}(G_n - 1)(u_p)|,$$

so we need only work with $D_{p,n}(G_n - 1)(u_p)$. Now, we note that

$$D_{p,n}(G_n - 1)(u_p) = \frac{\eta_p(Q_{p,n-1}(1))}{\eta_p(Q_{p,n}(1))} D_{p,n-1}(Q_n\{G_n - 1\})(u_p).$$

Now by using (A1) 1. we have

$$\frac{\eta_p(Q_{p,n-1}(1))}{\eta_p(Q_{p,n}(1))} \leq C. \quad (\text{A.4})$$

In addition

$$M_n(G_n - 1)(u_{n-1}) = \int_{\mathbf{E}_n} \left(\frac{p_{n+1}(y_{1:N}|u_n)}{p_n(y_{1:N}|\bar{u}_{n-1})} - 1 \right) M_n(u_{n-1}, du_n),$$

where we use the notation $u_n = (\bar{u}_{n-1}, \tilde{\theta}_{n+1}) \in \mathbf{E}_n$. Now by using (A1) 1. followed by (A1) 4. and then (A1) 5.

$$|M_n(G_n - 1)(u_{n-1})| \leq C \int_{\mathbf{E}_n} |f_{n+1}(x, u_n) - f_n(x, \bar{u}_{n-1})| M_n(u_{n-1}, du_n) \leq C n_l^{-\beta/2}. \quad (\text{A.5})$$

Therefore, we have

$$D_{p,n}(G_n - 1)(u_p) = \frac{\eta_p(Q_{p,n-1}(1))}{\eta_p(Q_{p,n}(1))} D_{p,n-1} \left(\frac{Q_n\{G_n - 1\}}{\|Q_n\{G_n - 1\}\|_\infty} \right) (u_p) \|Q_n\{G_n - 1\}\|_\infty,$$

where for any $\varphi_p \in \mathcal{B}_b(\mathbf{E}_p)$, $\|\varphi_p\|_\infty = \sup_{u_p \in \mathbf{E}_p} |\varphi_p(u_p)|$. Application of (A.4) and [5, Lemma A.1. (i)] yields

$$|D_{p,n}(G_n - 1)(u_p)| \leq C \zeta^{n-p} \|Q_n\{G_n - 1\}\|_\infty.$$

Then using (A1) 1. and (A.5) yields

$$\sup_{u_p \in \mathbf{E}_p} |D_{p,n}(\varphi_n)(u_p)| \leq C \zeta^{n-p} n_l^{-\beta/2}.$$

For the proof of 2. the case $0 \leq p < n$ follows immediately from 1. and the proof in [5, Lemma A.1. (ii)]. So we need only consider $n = p$, which reads

$$\sqrt{P_n} \mathbb{E}[|[\eta_n^{P_n} - \Phi_n(\eta_{n-1}^{P_{n-1}})](\varphi_n)|^r]^{1/r},$$

and then using (A.3) we need only consider

$$\sqrt{P_n} \mathbb{E}[|[\eta_n^{P_n} - \Phi_n(\eta_{n-1}^{P_{n-1}})](G_n - 1)|^r]^{1/r}.$$

Using the conditional Marcinkiewicz-Zygmund inequality gives the upper-bound

$$\|V_n(D_{n,n}(\varphi_n))\|_r \leq C \mathbb{E}[|G_n(U_n^1) - 1|^r]^{1/r}.$$

Taking conditional expectations w.r.t. M_n and using (A.5) yields

$$\|V_n(D_{n,n}(\varphi_n))\|_r \leq C n_l^{-\beta/2},$$

which is the desired result.

For the proof of 3. this follows immediately from 1. and the proof in [5, Lemma A.1. (iii)]. \square

Remark A.1. Given the results in Lemma A.1, one can follow the proofs of [5, Theorem 3.1.] to deduce that for any $j \in \{1, 2, 3\}$

$$\mathbb{E}[(\sum_{l=2}^L T_j^{P_{l-1}})^2] \leq C \left(\sum_{l=2}^L \frac{1}{P_{l-1} n_l^\beta} + \sum_{2 \leq l < q \leq L} \frac{1}{(n_l n_q)^{\beta/2}} \left\{ \frac{\zeta^{q-1}}{P_{l-1}} + \frac{1}{P_{l-1}^{1/2} P_{q-1}} \right\} \right),$$

with the notations as in the statement of Proposition 3.1.

References

- [1] Devanshu Agrawal, Theodore Papamarkou, and Jacob D. Hinkle. Wide neural networks with bottlenecks are deep Gaussian processes. *J. Mach. Learn. Res.*, 21:1–66, 2020.
- [2] Andrew R Barron. Universal approximation bounds for superpositions of a sigmoidal function. *IEEE Transactions on Information theory* 39 (3), 930-945, 1993.
- [3] Jason M Klusowski and Andrew R Barron. Approximation by Combinations of ReLU and Squared ReLU Ridge Functions With ell^1 and ell^0 Controls, *IEEE Transactions on Information Theory*, 64:12, 7649–7656, 2018.
- [4] Dimitri P. Bertsekas. *Dynamic Programming and Optimal Control*. Athena Scientific, 1985.
- [5] Alexandros Beskos, Ajay Jasra, Kody J. H. Law, Raul Tempone, and Yan Zhou. Multilevel sequential Monte Carlo samplers. *Stochastic Processes and their Applications*, 127(5):1417–1440, 2017.
- [6] Alexandros Beskos, Ajay Jasra, Kody J. H. Law, Youssef Marzouk and Yan Zhou. Multilevel sequential Monte Carlo with dimension independent likelihood informed proposals. *SIAM/ASA Journal on Uncertainty Quantification*, 6:762–786, 2018.
- [7] Christopher M. Bishop. *Pattern recognition and machine learning (information science and statistics)*, 2006.
- [8] David M Blei, Alp Kucukelbir, and Jon D McAuliffe. Variational inference: A review for statisticians. *Journal of the American statistical Association*, 112:518, 859–877, 2017.
- [9] Pierre Del Moral. *Feynman-Kac Formulae*. Springer, 2004.
- [10] Pierre Del Moral, Arnaud Doucet and Ajay Jasra. Sequential Monte Carlo samplers. *Journal of the Royal Statistical Society: Series B (Statistical Methodology)*, 68(3), 411–436, 2006.
- [11] Pierre Del Moral, Arnaud Doucet and Ajay Jasra. On adaptive resampling strategies for sequential Monte Carlo methods. *Bernoulli*, 18:252–278, 2012.
- [12] Matthew M. Dunlop, Mark A. Girolami, Andrew M. Stuart, Aretha L. Teckentrup. How deep are deep Gaussian processes? *J. Mach. Learn. Res.*, 19 (54), 1–46, 2018.
- [13] Matthew M. Dunlop, Chen Li and Georg Stadler. Bayesian neural network priors for edge-preserving inversion. *arXiv preprint [arXiv:2112.10663](https://arxiv.org/abs/2112.10663)*, 2021.
- [14] Weinan E, Jiequn Han and Arnulf Jentzen. Algorithms for solving high dimensional PDEs: from nonlinear Monte Carlo to machine learning. *Nonlinearity* 35, 278–310, 2022.
- [15] Masahiro Fujisawa and Issei Sato. Multilevel Monte Carlo variational inference. *J. Mach. Learn. Res.*, 22, 1-44, 2021.
- [16] Yarin Gal and Zoubin Ghahramani. Dropout as a Bayesian approximation: Representing model uncertainty in deep learning. *International Conference on Machine Learning*, 1050–1059, 2016.
- [17] Charles Blundell, Julien Cornebise, Koray Kavukcuoglu and Daan Wierstra. Weight uncertainty in neural network. *International Conference on Machine Learning*, 1613–1622, 2015.
- [18] Michael B. Giles. Multilevel Monte Carlo path simulation. *Op. Res.*, 56, 607–617, 2008.
- [19] Michael B. Giles. Multilevel Monte Carlo methods. *Acta Numerica*, 24, 259–328, 2015.
- [20] Thomas Gerstner, Bastian Harrach, Daniel Roth and Martin Simon. Multilevel Monte Carlo learning. *Arxiv preprint [arXiv:2102.08734](https://arxiv.org/abs/2102.08734)*, 2021.

- [21] Katherine A. Heller and Zoubin Ghahramani. Bayesian hierarchical clustering. *Proceedings of the 22nd international conference on Machine learning*, 297–304, 2005.
- [22] Ian Goodfellow, Yoshua Bengio, and Aaron Courville. *Deep learning*. MIT press, 2016.
- [23] Abdul Lateef Haji-Ali, Fabio Nobile and Raul Tempone. Multi-index Monte Carlo: when sparsity meets sampling. *Numerische Mathematik*, 132(4), 767–806, 2016.
- [24] Trevor Hastie, Robert Tibshirani and Jerome H. Friedman. *The Elements of Statistical Learning*. Springer, 2001.
- [25] Douglas Heaven. Why deep-learning AIs are so easy to fool. *Nature* 574.7777, 163–166, 2019.
- [26] Stefan Heinrich. Multilevel Monte Carlo methods. In *Large-Scale Scientific Computing*, (eds. S. Margenov, J. Wasniewski & P. Yalamov), Springer, 2001.
- [27] Jeremy Heng, Ajay Jasra, Kody J. H. Law, and Alexander Tarakanov. On unbiased estimation for discretized models. *arXiv preprint [arXiv:2102.12230](https://arxiv.org/abs/2102.12230)*, 2021.
- [28] Kurt Hornik, Maxwell Stinchcombe and Halbert White. Multilayer Feedforward Networks are Universal Approximators. *Neural Networks. Vol. 2*. 359–366, 1989.
- [29] Ajay Jasra, Chris C. Holmes and David A. Stephens. MCMC methods and the label switching problem in Bayesian mixture modelling. *Stat. Sci.*, 20, 50–67, 2005.
- [30] Ajay Jasra, Kengo Kamatani, Kody J. H. Law and Yan Zhou. Multilevel particle filters. *SIAM J. Numer. Anal.*, 55(6), 3068–3096, 2017.
- [31] Ajay Jasra, Kody J. H. Law, and Deng Lu. Unbiased estimation of the gradient of the log-likelihood in inverse problems. *Statistics and Computing*, 31(3):1–18, 2021.
- [32] Andreas Damianou, Neil D Lawrence. Deep Gaussian processes. *Artificial Intelligence and Statistics*, 207-215, 2013.
- [33] Jaehoon Lee, Yasaman Bahri, Roman Novak, Samuel S. Schoenholz, Jeffrey Pennington, and Jascha Sohl-Dickstein. Deep neural networks as gaussian processes. In *International Conference on Learning Representations*, 2018.
- [34] Kjetil O. Lye, Siddhartha Mishra and Roberto Molinaro. A multi-level procedure for enhancing accuracy of machine learning algorithms. *Euro. Journal of Applied Mathematics*, 32(3), 436–469, 2021.
- [35] David J. C. MacKay. *Information theory, inference and learning algorithms*. Cambridge university press, 2003.
- [36] Alexander G de G Matthews, Jiri Hron, Mark Rowland, Richard E. Turner, and Zoubin Ghahramani. Gaussian process behaviour in wide deep neural networks. In *International Conference on Learning Representations*, 2018.
- [37] Seyed-Mohsen Moosavi-Dezfooli, Alhussein Fawzi, and Pascal Frossard. Deepfool: a simple and accurate method to fool deep neural networks. *Proceedings of the IEEE conference on computer vision and pattern recognition*, 2574–2582, 2016.
- [38] K Monterrubio-Gómez, L Roininen, S Wade, T Damoulas, and M Girolami. Posterior inference for sparse hierarchical non-stationary models. *Computational Statistics & Data Analysis* 148, 106954, 2020.
- [39] Kevin P. Murphy. *Probabilistic Machine Learning*. MIT Press, 2022.

- [40] Radford M Neal. *Bayesian learning for neural networks*, volume 118. Springer Science & Business Media, 2012.
- [41] Gabriel Lord, Catherine.E. Powell and Tony Shardlow. *An Introduction to Computational Stochastic PDEs*. Cambridge Texts in Applied Mathematics, 2014.
- [42] Deepak Ramachandran and Eyal Amir. Bayesian inverse reinforcement learning. *IJCAI*, 7, 2586–2591, 2007.
- [43] Torben Sell and Sumeetpal S. Singh. Dimension-robust function space mcmc with neural network priors. *arXiv preprint [arXiv:2012.10943](https://arxiv.org/abs/2012.10943)*, 2020.
- [44] Yuyang Shi, Rob Cornish. On multilevel Monte Carlo unbiased gradient estimation for deep latent variable models. *Proceedings of The 24th International Conference on Artificial Intelligence and Statistics, PMLR130:3925–3933*, 2021.
- [45] Emanuel Todorov, Tom Erez, and Yuval Tassa. Mujoco: A physics engine for model-based control. *IEEE/RSJ International Conference on Intelligent Robots and Systems, pages 5026-5033*. IEEE, 2012.
- [46] Zhiqing Xiao. *Reinforcement Learning: Theory and Python Implementation*. China Machine Press, 2019.